Membrane Interactions of Mutated Forms of the Influenza Fusion Peptide†

Richard M. Epand,*,‡ Raquel F. Epand,‡ Isabelle Martin,§ and Jean-Marie Ruysschaert§

Department of Biochemistry, McMaster University, Hamilton, Ontario, Canada L8N 3Z5, and Structure et Fonction des Membranes Biologiques (SFMB), CP206/2, Université Libre de Bruxelles, 1050 Brussels, Belgium

Received April 9, 2001; Revised Manuscript Received May 29, 2001

ABSTRACT: We have studied a group of fusion peptides of influenza hemagglutinin in which the N-terminal amino acid, Gly (found in the wild-type peptide), has been systematically substituted with Ala, Ser, Val, or Glu. The activity of the intact hemagglutinin protein with these same substitutions has already been reported. As a measure of the extent of modulation of intrinsic membrane curvature by these peptides, we determined their effects on the polymorphic phase transition of dipalmitoleoylphosphatidylethanolamine. The wild-type peptide is the only one that, at pH 5, can substantially decrease the temperature of this transition. This is also the only form in which the intact protein promotes contents mixing in cells. The Ala and Ser mutant hemagglutinins exhibit a hemifusion phenotype, and their fusion peptides have little effect on lipid polymorphism at low pH. The two mutant proteins that are completely fusion inactive are the Val and Glu mutant hemagglutinins. The fusion peptides from these forms significantly increase the polymorphic phase transition temperature at low pH. We find that the effect of the fusion peptides on membrane curvature, as monitored by a shift in the temperature of this polymorphic phase transition, correlates better with the fusogenic activities of the corresponding protein than do measurements of the isotropic ^{31}P NMR signals or the ability to induce the fusion of liposomes. The inactivity of the hemagglutinin protein with the hydrophobic Val mutation can be explained by the change in the angle of membrane insertion of the helical fusion peptide as measured by polarized FTIR. Thus, the nature of the interactions of the fusion peptides with membranes can, in large part, explain the differences in the fusogenic activity of the intact protein.

The fusion of influenza virus to target membranes is one of the most extensively studied viral fusion processes. As with several other enveloped viruses, there is a short segment of the viral fusion protein, termed the fusion peptide, which is essential for viral fusion. The fusion peptide of influenza, as with several other viruses, is found at a newly formed amino terminus as a consequence of activation of the viral fusion protein by proteolysis. It is this segment of the fusion protein that inserts into target membranes (*1*). Another indication that this segment is important for fusion is that mutations within this region lead to loss of fusogenic activity. It had long been known, for example, that replacement of the Gly residue at position 1 of the fusion peptide with Glu resulted in a fusion inactive virus (*2*). A high Gly content is a common feature of fusion peptides. It may play a role in causing the fusion peptide to enter the membrane at an oblique angle, a condition thought to be important for fusogenic activity (*3*). It has been shown that the 20-amino acid fusion peptide of influenza virus also inserts into a membrane as a tilted helix (*4*). A modified form of this fusion peptide, designed to be more soluble in water and therefore more experimentally tractable, is also inserted into membranes as a tilted helix (*5*). The role of some of the hydrophobic residues in this modified peptide has also been studied (*6*). Molecular modeling studies of a number of the influenza fusion peptides indicate that oblique insertion of the peptide into a membrane is the most important factor in determining fusogenicity (*7*).

The presence of the fusion peptide in the influenza hemagglutinin appears to be essential for rapid viral fusion, but there are other segments of the ectodomain of the viral fusion protein that can greatly enhance fusogenic activity (*8*). It has been suggested that a viral fusion protein can partially unfold during the fusion process to orient other helical regions at the membrane interface (*9*). In addition, both the transmembrane and intraviral domains of the viral fusion protein can participate in membrane fusion (*10*).

Promotion of negative curvature by the viral fusion peptide (*11*) in the cis or contacting monolayer will facilitate the formation of a stalk or hemifusion intermediate. To evolve from a hemifusion intermediate to a fusion pore, the trans monolayer has to adopt positive curvature (*12*). At higher peptide-to-lipid ratios, the influenza fusion peptide promotes the formation of a bicontinuous cubic phase (*13*, *14*). The mechanism of formation of a bicontinuous cubic phase is thought to be similar to the mechanism of formation of membrane fusion intermediates. The role of the influenza fusion peptide in facilitating fusion pore opening is thought to be unrelated to changes in membrane curvature (*14*).

† This work was funded by Grant MT-7654 from the Canadian Institutes of Health Research (R.M.E.) and by FNRS and ARC (Actions de Recherches Concertées) (J.-M.R.).

* To whom correspondence should be addressed. E-mail: epand@mcmaster.ca. Telephone: (905) 525-9140, ext 22073. Fax: (905) 521-1397.

‡ McMaster University.

§ Université Libre de Bruxelles.

10.1021/bi0107187 CCC: $20.00
Published on Web 06/28/2001

The influenza hemagglutinin protein is comprised of two disulfide-linked polypeptide chains, HA1 and HA2. The HA1 subunit contains the sialic acid receptor binding domain, while the HA2 subunit is the fusogenic component and contains the fusion peptide at the N-terminus. Recently, a series of mutated forms of the influenza hemagglutinin protein in which the N-terminal amino acid of the HA2 subunit has been replaced has been studied. The amino acid Gly, normally at this position, was substituted with a polar and charged residue, Glu; a polar and uncharged residue, Ser; a more hydrophobic and bulky amino acid, Val; and the natural amino acid most similar to Gly, i.e., Ala. These mutated proteins exhibited a range of activities from being totally fusion inactive, to promoting only hemifusion, and finally to forms which exhibit full fusion activity (*15*). We have made a series of 20-amino acid fusion peptides, corresponding to segments of these mutated hemagglutinin proteins from the X-31 strain of influenza virus. The sequence of this fusion peptide for the wild-type protein i: GLFGAIAGFIENGWEGMIDG-amide with the mutant forms having A, S, V, or E substituted at position 1. We have tested the ability of these isolated fusion peptides to promote fusion in liposomal systems as well as to promote negative curvature in membranes and to affect the morphology of lipid aggregates as assessed using ^{31}P NMR. In addition, we have employed FTIR methods to analyze the conformation and mode of insertion of the most hydrophobic peptide that was fusion inactive. These measurements, by their nature, require the use of different lipid systems. Our comparisons focus on the differences among the various forms of the fusion peptide and not on comparison of results from different assays systems for one particular peptide.

MATERIALS AND METHODS

Materials. All lipids, including the fluorescently labeled lipids, were purchased from Avanti Polar Lipids (Alabaster, AL). The peptides were synthesized by Biosource (Hopkinton, MA) and purified to >95% purity by HPLC.

Differential Scanning Calorimetry (DSC).[1] Lipid films were made from DiPoPE, and to some tubes were also added small aliquots of a peptide from a dilute methanolic solution. The lipid films were suspended either in 20 mM PIPES, 1 mM EDTA, and 150 mM NaCl with 0.002% NaN_3 (pH 7.40) or in 10 mM sodium citrate buffer, 1 mM EDTA, and 140 mM NaCl (pH 5.0) by vortexing at room temperature. The final lipid concentration was 7.5 mg/mL. The lipid suspension was degassed under vacuum before being loaded into a NanoCal high-sensitivity scanning calorimeter (CSC, Provo, UT). A heating scan rate of 0.75 °C/min was employed. The bilayer to hexagonal phase transition was fitted using parameters to describe equilibrium with a single van't Hoff enthalpy and the transition temperature determined as that for the fitted curve. Data were analyzed with the program Origin. The calculated transition temperatures were then plotted as a function of the mole fraction of fusion peptide and the slope of this plot reported in Table 1. A positive value of this parameter indicates that the peptide is increasing T_H, suggesting that it is promoting positive membrane curvature, while a negative value indicates the opposite.

Table 1: Influenza Fusion Peptide

	virus		liposomes		
N-terminus	lipid mixing	contents mixing	T_H at pH 7 (°C/mole fraction)[a]	T_H at pH 5 (°C/mole fraction)[a]	lipid mixing
Gly	+	+	301 ± 49	−453 ± 112	+
Ala	+	±	274 ± 70	55 ± 73	−
Ser	+	−	88 ± 20	72 ± 89	−
Val	−	−	400 ± 53	320 ± 80	±
Glu	−	−	734 ± 228	525 ± 200	−

[a] Values are obtained from a linear regression analysis of a plot of T_H vs mole fraction of peptide.

^{31}P NMR. The ^{31}P NMR spectra were measured using suspensions of ~15 mg of DiPoPE with or without the addition of 1 mol % peptide. The lipid and peptide were mixed in organic solvent and dried, as described for DSC. The lipid film was hydrated with 10 mM sodium citrate buffer, 1 mM EDTA, and 140 mM NaCl (pH 5.0). Spectra were obtained using a Bruker AM-500 spectrometer operating at 202.45 MHz in a 10 mm broad-band probe over a 30 kHz sweep width in 16 × 1024 data points. A 90° pulse width of 16.6 μs was used. Composite pulse decoupling was used to remove any proton coupling. Generally, 800 free induction decays were processed using an exponential line broadening of 100 Hz prior to Fourier transformation. The probe temperature was maintained within ±0.2 °C by a Bruker B-VT 1000 variable-temperature unit. Temperatures were monitored with a calibrated thermocouple probe placed in the cavity of the NMR magnet.

Lipid Mixing Assay for Membrane Fusion. The resonance energy transfer assay of Struck et al. (*16*) was used to monitor membrane fusion. LUV were prepared containing DOPC, DOPE, and cholesterol at a molar ratio of 1:1:1. For each of these lipid systems, two populations of LUV were prepared, one unlabeled and one labeled with N-Rh-PE and N-NBD-PE (2 mol % each). A 9:1 molar ratio of unlabeled to labeled liposomes was used in the assay. Fluorescence was recorded at excitation and emission wavelengths of 465 and 530 nm, respectively, using a 490 nm cutoff filter placed between the cuvette and the emission monochromator, with 4 nm bandwidths, using an SLM Aminco Bowman AB-2 spectrofluorimeter. Siliconized glass cuvettes (1 cm^2) were used with continuous stirring in a thermostated cuvette holder. Measurements were carried out using a buffer containing 5 mM Hepes, 5 mM Mes, 5 mM citric acid, 0.15 M NaCl, and 1 mM EDTA (pH 7.0). LUV at a final lipid concentration of 50 or 100 μM were added to 2 mL of buffer in the cuvette at 37 °C, and then the peptide was injected from a solution of DMSO. The solution was then acidified to pH 5.0 by the addition of 10 μL of 1 mM citric acid. Fluorescence was recorded for several minutes, and then 20 μL of 10% Triton X-100 was added (final concentration of 0.1%). The initial residual fluorescence intensity, prior to acidification, F_o, was taken to be zero. The maximum fluorescence intensity, F_{max}, was obtained by dilution of the labeled lipids with 20 μL of 10% Triton X-100. The percent lipid mixing at time *t* is given

[1] Abbreviations: DSC, differential scanning calorimetry; DiPoPE, dipalmitoleoylphosphatidylethanolamine; DOPC, dioleoylphosphatidylcholine; DOPE, dioleoylphosphatidylethanolamine; T_H, bilayer to hexagonal phase transition temperature; N-Rh-PE, *N*-(lissamine rhodamine B sulfonyl)phosphatidylethanolamine; N-NBD-PE, *N*-(7-nitro-2,1,3-benzoxadiazol-4-yl)phosphatidylethanolamine; LUV, large unilamellar vesicles; ATR-FTIR, attenuated total reflection Fourier transform infrared spectroscopy.

by $[(F_t - F_o)/(F_{max} - F_o)] \times 100$. All runs were carried out in duplicate and were found to be in close agreement. Controls were done using comparable volumes of DMSO in the absence of peptide. The intensity of maximal fluorescence with Triton was found to be close to that obtained when the mole fraction of labeled lipids was reduced by 10-fold with unlabeled lipid and was taken to be the fluorescence corresponding to 100% fusion.

Attenuated Total Reflection Fourier Transform Infrared Spectroscopy (ATR-FTIR). Routinely, lipids were dissolved in chloroform at the desired concentrations, and the solution was dried under a stream of nitrogen to deposit a thin lipid film on the inside of a glass test tube. The film was further subjected to vacuum evaporation for 2−3 h to remove any trace of the solvent. Large unilamellar vesicles (LUV) were prepared by hydrating the dried lipid film with the Hepes buffer [10 mM Hepes, 150 mM NaCl, 0.1 mM EDTA, and 0.02% NaN_3 (pH 7.2)], then repeatedly freezing and thawing the suspension five times, and finally extruding it 10 times through two polycarbonate filters with a pore size of 0.1 μm (Nucleopore Corp., Pleasanton, CA) using an extruder (Lipex Biomembranes Inc., Vancouver, BC). The prepared liposomes were stored at 4 °C until they were used. The fusion peptide dissolved in methanol was added to the liposome preparation at a 1:100 peptide:lipid ratio, or for pure peptide samples, the peptide was deposited directly on the germanium plate by evaporation of the methanolic solution.

Spectra were recorded at room temperature on a Perkin-Elmer 1720X FTIR spectrophotometer equipped with a liquid nitrogen-cooled mercury cadmium telluride (MCT) detector at a nominal resolution of 4 cm^{-1}, and encoded every 1 cm^{-1} (*17*). The spectrophotometer was continuously purged with air, which had been dried on a silica gel column. The internal reflection element was a germanium plate (50 mm × 50 mm × 2 mm, Harrick EJ2121) with an aperture angle of 45°, yielding 25 internal reflections. For each spectrum, 128 scan cycles were averaged; in each cycle, the sample spectra were ratioed against the background spectra of a clean germanium plate, using a shuttle to move the sample or reference into the beam. For polarization experiments, a Perkin-Elmer gold wire grid polarizer was positioned before the sample and the reference.

Oriented multilayers were obtained by slow evaporation under a N_2 stream at room temperature on one side of the germanium plate. To differentiate between the α-helix and the random structures, the multilayers were exposed for 3 h to D_2O-saturated N_2.

Orientation of the Secondary Structure. ATR-FTIR allows spectra to be recorded on ordered lipid bilayers, and information can be gained about the orientation of different structures within proteins or peptides with respect to the bilayer. In an α-helix, the main transition dipole moment (C═O) is almost parallel to the helix axis, while in an antiparallel β-sheet, the polarization is opposite, predominantly perpendicular to the fiber axis. It is therefore possible to determine the mean orientation of the α-helix and β-sheet structures from the orientation of the peptide bonds corresponding to those of the C═O groups. Spectra were recorded with parallel (0°) and perpendicular (90°) polarized incident light with respect to the ATR plate. The difference spectra are obtained by subtracting the 0° polarization spectrum from the 90° polarization spectrum normalized to each other by zeroing the net integral of the intensities of the ester C═O stretching band of the *sn*-1 and *sn*-2 lipid chains in the 1710−1760 cm^{-1} region in the difference spectrum. The rationale behind this lies in the fact that both the *sn*-1 and *sn*-2 carbonyl groups are found to make angles with respect to the bilayer normal that are close to the value for an isotropic orientation and their IR intensities are therefore expected to be independent of the polarization. Dichroic ratios were calculated as described previously (*17*).

Kinetics of Deuteration. The oriented multilayers were obtained by slow evaporation of the liposomes under a N_2 stream, on a germanium plate as described above. Before the deuteration was started, 10 spectra were recorded to verify the reproducibility of the measurements and the stability of the system. At time zero, a D_2O-saturated N_2 flux was applied to the sample with a flow rate of 100 mL/min, controlled with a Brooks flow meter. The spectra at each time point were recorded on a Bruker IFS55 FTIR spectrophotometer and were the accumulation of 24 scans, with a resolution of 4 cm^{-1}. The amide I and II band areas were measured between 1700 and 1600 cm^{-1} and between 1585 and 1502 cm^{-1}, respectively. The amide II area was divided by the amide I area for each spectrum to correct for any change in total intensity of the spectra during the deuteration process. This ratio, expressed between 0 and 100%, was plotted versus deuteration time. The 100% value is defined by the amide II:amide I ratio obtained before deuteration, whereas the 0% value corresponds to a zero absorption in the amide II region. It has been shown previously on a series of proteins that can be fully denatured (and therefore fully deuterated) and then refolded to their native conformation, that complete H/D exchange results in a 0−5% absorption intensity in the amide II region. We are therefore confident that a zero absorbance in the amide II region corresponds to full deuteration of the protein.

RESULTS

We have summarized both the results of studies of the wild-type and mutated hemagglutinin on cell membranes (*15*) and some of our results with the model fusion peptide affecting liposome systems (Table 1). The N-terminus corresponds to the amino acid at position 1 in the 20-amino acid fusion peptide, whose full sequence is given in the introductory section. Gly is the amino acid found in the wild-type protein. The shift in T_H with mole fraction of peptide is given in columns 4 and 5 of Table 1. At pH 7, all of the peptides increase T_H, with the Glu^1 mutant having the strongest effect. This would be in accord with its greater polarity and thus less penetration into the membrane. We cannot explain why the Ser^1 mutant shifts T_H by a much smaller amount at pH 7, compared with the other peptides. A contributing factor could be a lower level of membrane partitioning of this peptide. However, all of the fusion peptides that were studied were very sparsely soluble in water, making it difficult to determine the partition coefficients. In addition, because of the low water solubility one would anticipate that the peptide is largely partitioned into the membrane. Furthermore, the measured phase transition is broadened by all of the peptides to a comparable extent, again indicating partitioning of the peptide into the membrane. Thus, although differences in partitioning may con-

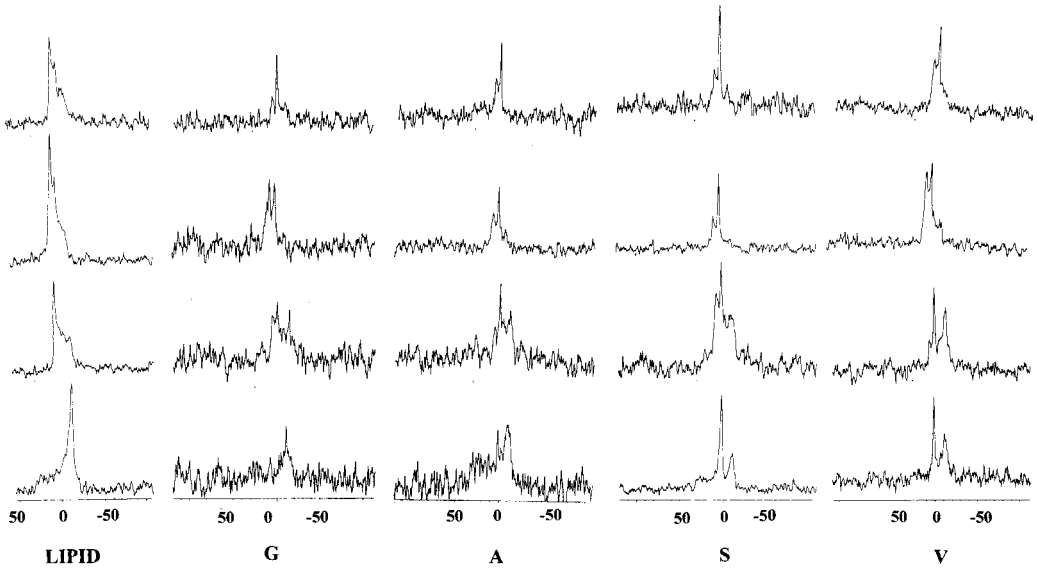

FIGURE 1: ^{31}P NMR spectra of DiPoPE with and without the addition of 1 mol % peptide as a function of temperature. All samples contain 15 mg of DiPoPE. The samples were hydrated with 10 mM sodium citrate buffer, 1 mM EDTA, and 140 mM NaCl (pH 5.0).

tribute to the magnitude of the effect of the peptide on the lipid phase transition, it will not affect the direction of the shift in the transition temperature, i.e., to higher or to lower values. The differences in the effects of the peptides on T_H are even more pronounced at pH 5. At this acidic pH, only the Gly^1 peptide significantly decreases T_H. Interestingly, the other two mutant forms, Ala^1 and Ser^1, that allow lipid mixing in cell systems at acidic pH do not significantly increase T_H, as do the two completely inactive mutant hemagglutinin proteins containing Val^1 or Glu^1. Thus, there is a good correlation between the direction of the shift of T_H caused by the fusion peptide and the fusogenic activity of the corresponding intact hemagglutinin protein.

Another method for assessing the conversion of the bilayer phase to an inverted phase is by measuring ^{31}P NMR powder patterns of the phospholipid. In addition to detecting lamellar and hexagonal phases, this method will also monitor the presence of structures of high curvature, giving rise to isotropic ^{31}P NMR signals. Such isotropic signals have been associated with more rapid rates of membrane fusion (*18*). The cubic phase is one type of structure that exhibits isotropic ^{31}P NMR signals. Because of the limited amount of peptide available and because it was difficult to maintain the aggregated peptide/lipid samples in an area of the NMR tube that could be detected by the receiving coil, the signal-to-noise ratio of the samples with peptide is poor. Nevertheless, it is clear that there is only a trace of isotropic signal with the pure lipid but that, in the presence of any of the peptides, there is a significant contribution from the isotropic signal (Figure 1). Isotropic ^{31}P NMR signals produced by the wild-type fusion peptide with monomethyldioleoylphosphatidylethanolamine had been observed previously (*19*). The quantitative contribution of the isotropic signal varies among the different peptides and also varies with temperature. The Ser^1 analogue is the most effective in inducing this property. There is no correlation between the size of the isotropic signal and the ability of the peptide to induce inverted phases (Table 1) or to promote liposome fusion (see below).

The Gly^1 form of the peptide is the most active in lipid mixing (Figure 2), and it is also the only form that allows

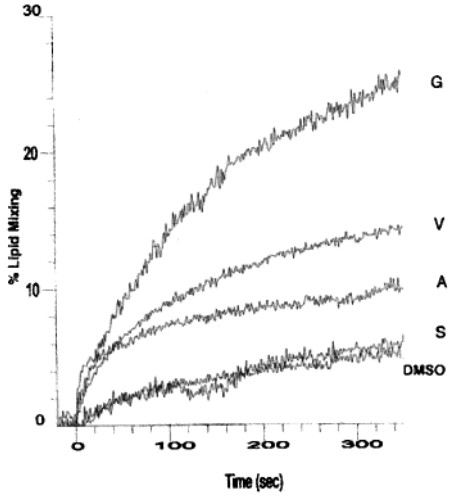

FIGURE 2: Promotion of lipid mixing by the fusion peptide at pH 5.0 using 50 μM LUV of DOPC, DOPE, and cholesterol (1:1:1). Curves show the activity of each of the indicated fusion peptides (all at 1 μM). The bottom curve is the DMSO control using volumes corresponding to that used with the peptide. The results for the Glu^1 mutant are not shown as they overlap with the curve for the Ala^1 mutant.

for efficient contents mixing in cell systems (Table 1). In addition, with the wild-type peptide, both the peptide-induced shifts in T_H and the fusogenic activity of the intact hemagglutinin protein and of the fusion peptide exhibit similar pH dependence. One would therefore anticipate that the mutant fusion peptides would also mimick the fusogenic activity with liposomes that the intact hemagglutinin protein has. This is the case for the wild-type peptide. However, the next most potent fusogen of liposomes is the Val^1 mutant (Figure 2) that increases, rather than decreases, T_H at acidic pH (Table 1). Thus, there is a poor correlation between the ability of the peptide to promote lipid mixing in liposomes and the effect of the peptide on membrane curvature or the effect of the same mutation on fusogenicity of the intact protein.

The most hydrophobic fusion peptide in the series is the Val^1 mutant. This peptide is therefore expected to penetrate most deeply into the membrane. This hydrophobicity,

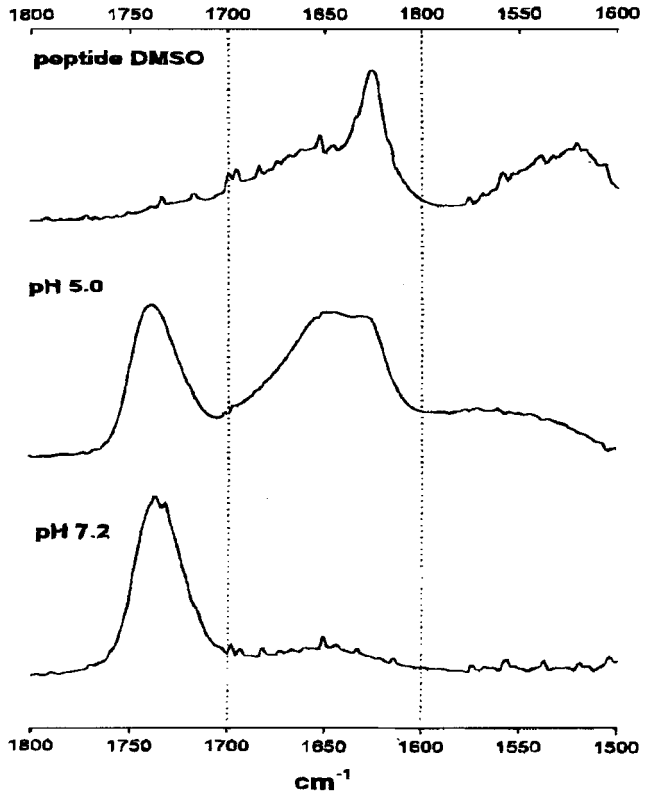

FIGURE 3: ATR-FTIR spectra between 1800 and 1500 cm^{-1} of the Val[1] fusion peptide in DMSO and associated with 1:1:1 PC/PE/PS LUV.

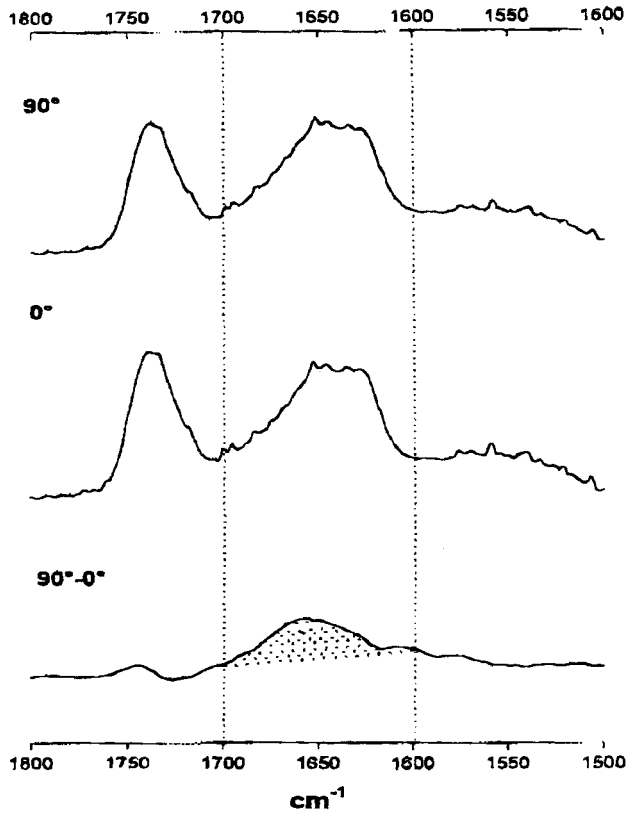

FIGURE 4: ATR dichroic spectrum of the Val[1] fusion peptide associated with 1:1:1 PC/PE/PS LUV. Spectra were recorded with 0° and 90° polarizations. The difference spectrum (90° − 0°) is normalized by zeroing the intensity of the ester C=O stretching bands of the *sn*-1 and *sn*-2 chains in the 1710−1760 cm^{-1} region of the difference spectrum. The dichroic spectrum was expanded 3-fold in the ordinate direction.

together with the bulkiness of the Val side chain, should cause the center of the bilayer to expand to a greater degree than the membrane interface, thus increasing negative intrinsic curvature. However, the peptide increases T_H, indicating that it is promoting positive curvature. Despite this, the Val[1] peptide is the most fusogenic of the mutant peptides, even though increased negative curvature is required for the initiation of membrane fusion and the formation of the stalk intermediate. We have therefore investigated the mode of insertion of this peptide in more detail using FTIR methods and have compared its properties with those of the wild-type peptide.

To obtain a significant fraction of the peptide inserting into the bilayer under the conditions of the FTIR experiments, it was necessary to incorporate bovine brain phosphatidylserine into the membrane. We do not know the reason for the requirement for phosphatidylserine, but it may relate to the fact that this is the only method used in this study that measures a structural feature that requires stable insertion of the peptide. It should be pointed out that the previous study with the wild-type influenza fusion peptide did not require addition of phosphatidylserine to the membrane to obtain peptide insertion. In comparison, the shift of T_H or the promotion of liposome fusion may be accomplished by a transient insertion of the peptide. The Val[1] mutant inserted as an α-helix into a membrane of egg phosphatidylcholine, egg phosphatidylethanolamine, and bovine brain phosphatidylserine (1:1:1 molar ratio) at neutral and acidic pH (Figure 3). The amide I band (1600−1700 cm^{-1}) is highly sensitive to the secondary structure (*17*), and its peak at 1650 cm^{-1} characterizes a high helical content. At pH 7.2, the magnitude of the amide I adsorption band is weak, suggesting that less peptide is bound to the membrane at this pH. This peptide has a lesser effect in promoting membrane fusion at this pH, in accord with this suggestion. It should be noted that loosely bound peptide was removed from the membrane prior to FTIR measurements and that the Val[1] mutant peptide did not adhere to the membrane as much as the wild-type fusion peptide did as indicated by the fact that the Val[1] mutant required the presence of phosphatidylserine to insert into the membrane. There is also a component in the spectrum that arises from a β-structure. It likely represents a fraction of the peptide that does not penetrate into the lipid bilayer since the β-structure is not oriented (see Figure 4, below). In DMSO, the Val[1] peptide adopted a β-structure.

We measured the orientation of the peptide in membranes using polarized FTIR. A positive deviation observed in the 1650 cm^{-1} region of the difference spectrum indicates that the α-helix of the Val mutant is mainly oriented parallel to the lipid acyl chains (Figure 4). The dichroic ratio of amide I band is 2 ± 0.1 and corresponds to an angle of 20° between the helix axis and a normal to the germanium plate. An angle of 27° between the transition dipole and the helix axis is taken into account as described previously (*17*). This is different from the wild-type fusion peptide that inserts into a membrane at an oblique angle (*4*). In this case, the absence of deviation observed in the difference spectrum corresponded to an intermediate oblique orientation that is neither parallel nor perpendicular to the lipid−water interface. The sensitivity of the angle of insertion to the nature of the

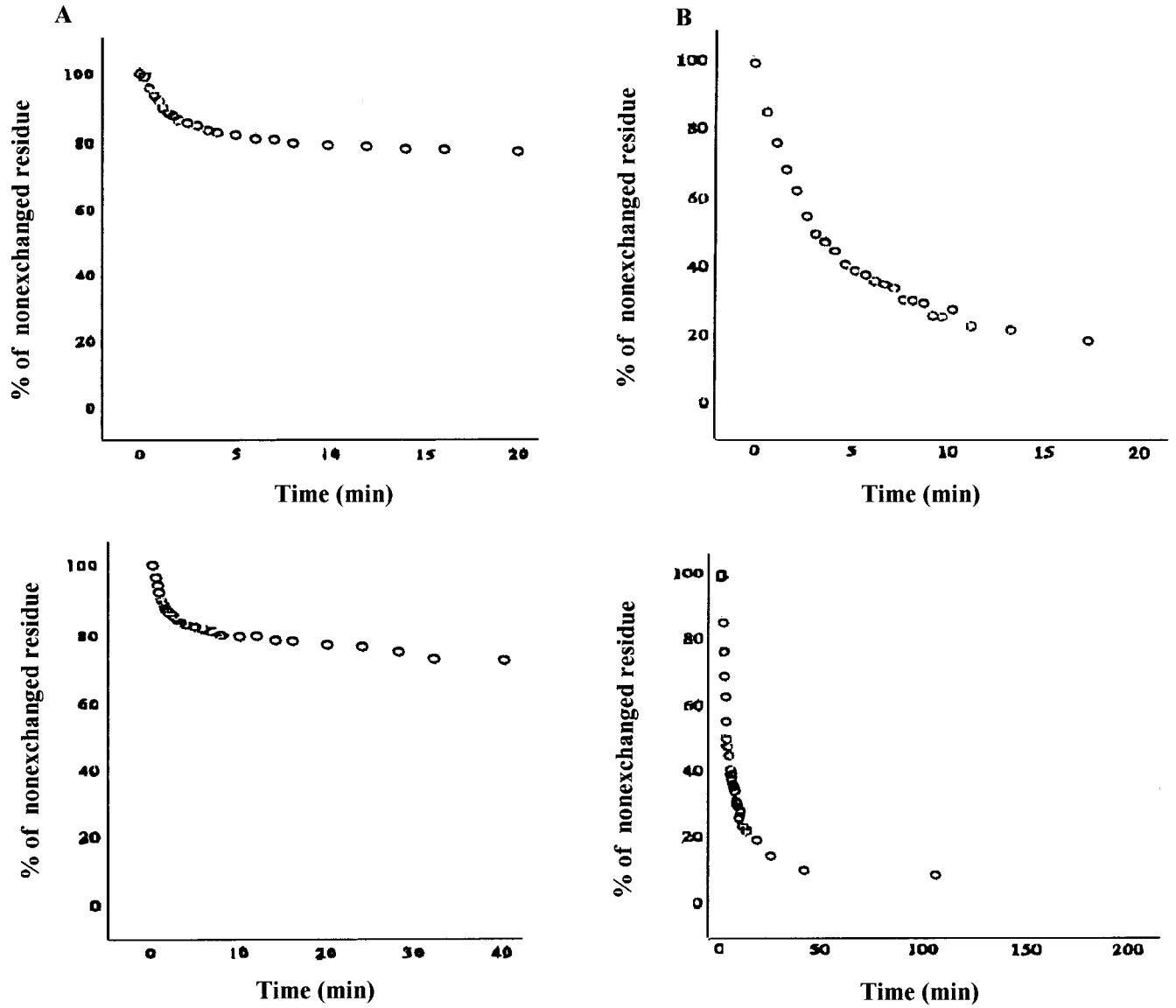

FIGURE 5: Evolution of the proportion of nonexchanged residues as a function of the deuteration time. The films were deposited on a germanium plate and exposed to a D_2O-saturated N_2 flux. The spectra were recorded with increasing time as described in Materials and Methods. (A) Val^1 fusion peptide in water. (B) Val^1 fusion peptide associated with 1:1:1 PC/PE/PS LUV. The top and bottom graphs illustrate different time scales.

N-terminal amino acid has been previously noted (*20*). The dichroic ratio of the δ-CH2 vibration at 1468 cm^{-1} is 1 ± 0.2. This means that the acyl chains of the lipid make a maximum tilt of 25° with respect to a normal to the germanium plate. Comparison of the helix axis and lipid acyl chain orientations demonstrates that they are parallel to each other.

The solvent accessibility of the amide bonds of the Val^1 mutant fusion peptide was measured using H/D exchange. In water, the peptide adopts a β-structure, and under this condition, the amide hydrogens are not accessible to exchange (Figure 5A). However, upon insertion into the membrane there is rapid exchange, with 80% of the amide hydrogens exchanging within 1 h (Figure 5B). This is in contrast to the wild-type peptide that shows no H/D exchange when incorporated into lipid (*21*).

DISCUSSION

There is a good correlation between the ability of the fusion peptide to decrease the T_H of DiPoPE and its ability to promote fusion when present at the amino terminus of the HA2 subunit of an intact hemagglutinin protein. The basis of this relationship is likely a consequence of the requirement of the cis monolayer for acquiring increased negative curvature in the stalk or hemifusion intermediate. There are three mutant hemagglutinin proteins that are active in hemifusion, i.e., Gly^1, Ala^1, and Ser^1. Although the fusion peptides from the latter two mutants are not as effective as the wild-type, Gly^1, fusion peptide in decreasing T_H, they do not increase T_H as do the Val^1 and Glu^1 mutant fusion peptides. The intact hemagglutinin proteins with the Val^1 and Glu^1 substitutions are inactive in lipid mixing. The peptide-promoted shifts in T_H correlate better with fusogenicity of the intact protein than do the appearance of fusion peptide-promoted isotropic ^{31}P NMR resonances or the ability of the fusion peptides to promote lipid mixing in liposomes. In addition, the only form of the hemagglutinin protein to promote efficient contents mixing is the wild type. The wild-type fusion peptide, with Gly, is also the only fusion peptide that can significantly decrease T_H at acidic pH. Thus, the

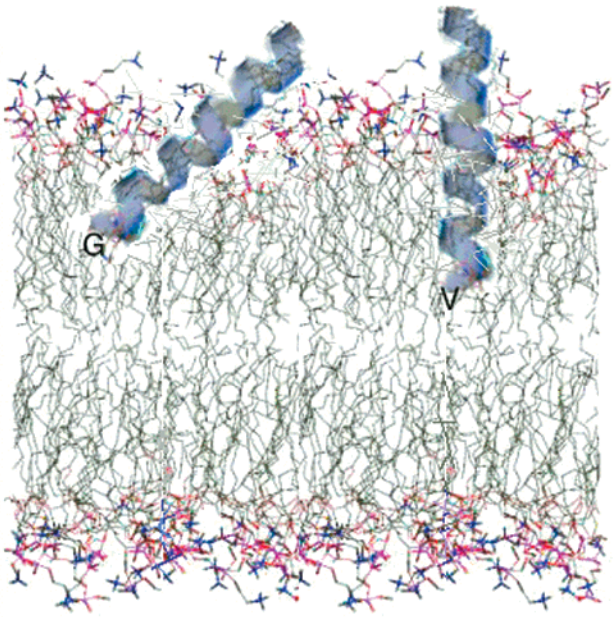

FIGURE 6: Schematic diagram illustrating the different orientations of the wild-type fusion peptide (with N-terminal G) and the Val[1] mutant. The orientations that are shown are based on the polarized ATR-FTIR studies. The model illustrates why rotation of the peptide around the bilayer normal results in much greater perturbation of acyl chain packing which would cause increased negative curvature strain.

ability to promote negative curvature may correlate with a property that can also affect steps in fusion after hemifusion.

A particularly interesting case is the Val[1] mutant. Although it is more hydrophobic than the wild-type peptide, the two peptides have almost the exact opposite effect on T_H at acidic pH. This can be explained as a result of a change in the orientation of the peptide helix with respect to the bilayer. As indicated by polarized FTIR, the wild-type peptide inserts into the membrane at an oblique angle, while the Val[1] mutant inserts along the bilayer normal. Peptides that orient along the bilayer normal expand the center of the bilayer less than those that insert at an oblique angle. As has been shown with SIV fusion peptides (*22*), this results in less negative curvature strain.

The wild-type influenza ectodomain of HA2 inserts into membranes with the amino-terminal end protruding further into the membrane (*23*), although the N-terminal Gly residue is still near the membrane interface (*24*). NMR analysis of the insertion of this peptide into SDS micelles also indicates that the amino terminus inserts more deeply (*25*). Substituting the N-terminal Gly with Val will allow this end of the peptide to partition into a more hydrophobic region of the membrane and thereby attain an orientation parallel to the bilayer normal. Interestingly, despite the greater depth of penetration of the Val[1] peptide, the exchange rates of the amide hydrogens are more rapid than they are with the wild-type peptide. We suggest that the greater penetration into the bilayer of bulky residues such as Val and Trp will result in packing defects within the bilayer, resulting in more facile penetration of water into the membrane and consequently faster exchange rates. This exposure of the hydrophobic regions of the membrane may also be responsible for the higher rate of lipid mixing by the Val[1] fusion peptide observed with liposomes (Figure 2). Such a mechanism of lipid mixing would not lead to complete fusion of two membranes. In the case of biological membranes, the perturbation of packing may be less important since these membranes have already accommodated a substantial fraction of their mass as proteins. Consequently, no lipid mixing is observed in the cell system with the intact hemagglutinin protein.

Thus, the property of decreasing T_H is a more reliable parameter for predicting the fusogenic activity of a viral fusion protein. There are obviously several differences between the intact hemagglutinin protein and the 20-amino acid N-terminal fusion peptide. There are other segments of the intact protein, in addition to the fusion peptide, that facilitate membrane fusion and other physical properties that also have to be considered. In addition, it is known that the self-association of the hemagglutinin protein is important for viral fusion. The self-association properties of the mutant proteins and their corresponding fusion peptides either in solution or in the membrane are not known. Nevertheless, there is very good correlation between the effects of the fusion peptide on membrane curvature and the fusogenicity of the intact protein, indicating that modulation of membrane curvature by the fusion peptide is at least a major contributing factor to the efficiency of membrane fusion. The results also illustrate the importance of the orientation of the inserted helix to the fusogenic activity of the intact protein. The most hydrophobic of the peptides studied was the Val[1] mutant. The fact that the Val[1] fusion peptide does not increase negative curvature can be explained on the basis of the orientation of the fusion peptide helix in a membrane (Figure 6). This also provides an explanation for why the intact Val[1] hemagglutinin protein is inactive in membrane fusion. It is thus possible to extrapolate from the curvature-modulating properties of this series of model peptides to the activity of the intact hemagglutinin proteins having the same amino acid replacements.

ACKNOWLEDGMENT

We are grateful to Dr. Donald Hughes for assistance in the measurement of the ^{31}P NMR spectra.

REFERENCES

1. Durrer, P., Galli, C., Hoenke, S., Corti, C., Gluck, R., Vorherr, T., and Brunner, J. (1996) *J. Biol. Chem. 271*, 13417−13421.
2. Gething, M. J., Doms, R. W., York, D., and White, J. (1986) *J. Cell Biol. 102*, 11−23.
3. Horth, M., Lambrecht, B., Khim, M. C., Bex, F., Thiriart, C., Ruysschaert, J. M., Burny, A., and Brasseur, R. (1991) *EMBO J. 10*, 2747−2755.
4. Luneberg, J., Martin, I., Nussler, F., Ruysschaert, J. M., and Herrmann, A. (1995) *J. Biol. Chem. 270*, 27606−27614.
5. Han, X., and Tamm, L. K. (2000) *Proc. Natl. Acad. Sci. U.S.A. 97*, 13097−13102.
6. Han, X., and Tamm, L. K. (2000) *J. Mol. Biol. 304*, 953−965.
7. Efremov, R. G., Nolde, D. E., Volynsky, P. E., Chernyavsky, A. A., Dubovskii, P. V., and Arseniev, A. S. (1999) *FEBS Lett. 462*, 205−210.
8. Epand, R. F., Macosko, J. C., Russell, C. J., Shin, Y. K., and Epand, R. M. (1999) *J. Mol. Biol. 286*, 489−503.
9. Shai, Y. (2000) *Biosci. Rep. 20*, 535−555.
10. Schroth-Diez, B., Ludwig, K., Baljinnyam, B., Kozerski, C., Huang, Q., and Herrmann, A. (2000) *Biosci. Rep. 20*, 571−595.
11. Epand, R. M. (1998) *Biochim. Biophys. Acta 1376*, 353−368.

12. Chernomordik, L. (1996) *Chem. Phys. Lipids 81*, 203−213.
13. Colotto, A., and Epand, R. M. (1997) *Biochemistry 36*, 7644−7651.
14. Siegel, D. P., and Epand, R. M. (2000) *Biochim. Biophys. Acta 1468*, 87−98.
15. Qiao, H., Armstrong, R. T., Melikyan, G. B., Cohen, F. S., and White, J. M. (1999) *Mol. Biol. Cell 10*, 2759−2769.
16. Struck, D. K., Hoekstra, D., and Pagano, R. E. (1981) *Biochemistry 20*, 4093−4099.
17. Goormaghtigh, E., Raussens, V., and Ruysschaert, J. M. (1999) *Biochim. Biophys. Acta 1422*, 105−185.
18. Ellens, H., Siegel, D. P., Alford, D., Yeagle, P. L., Boni, L., Lis, L. J., Quinn, P. J., and Bentz, J. (1989) *Biochemistry 28*, 3692−3703.
19. Epand, R. M., and Epand, R. F. (1994) *Biochem. Biophys. Res. Commun. 202*, 1420−1425.
20. Gray, C., Tatulian, S. A., Wharton, S. A., and Tamm, L. K. (1996) *Biophys. J. 70*, 2275−2286.
21. Razinkov, V., Martin, I., Turco, S. J., Cohen, F. S., Ruysschaert, J. M., and Epand, R. M. (1999) *Eur. J. Biochem. 262*, 890−899.
22. Epand, R. F., Martin, I., Ruysschaert, J. M., and Epand, R. M. (1994) *Biochem. Biophys. Res. Commun. 205*, 1938−1943.
23. Macosko, J. C., Kim, C. H., and Shin, Y. K. (1997) *J. Mol. Biol. 267*, 1139−1148.
24. Zhou, Z., Macosko, J. C., Hughes, D. W., Sayer, B. G., Hawes, J., and Epand, R. M. (2000) *Biophys. J. 78*, 2418−2425.
25. Chang, D. K., Cheng, S. F., Deo, T. V., and Yang, S. H. (2000) *J. Biol. Chem. 275*, 19150−19158.

BI0107187